scientific reports

Check for updates

OPEN

Advanced synthesis, comprehensive characterization, and potent cytotoxicity of 2,6-Bis(2-aminophenylimino) methyl)-4-methoxyphenol and its binuclear copper(II) complex

S. Praveen[1], R. Prabakarakrishnan[2], G. Parinamachivayam[3], A. Natarajan[4], Elumalai Perumal Venkatesan[8,10], K. Geetha[1]✉, Arunachalam Chinnathambi[5], Sulaiman Ali Alharbi[5], Arivalagan Pugazhendhi[6], Sabariswaran Kandasamy[7] & Nasim Hasan[9]✉

The imine base and Cu^{2+} precursors were combined using magnetic stirring to formulate the Cu^{2+} complexes. The formation of the imine base was confirmed by electronic and vibrational spectra, proton NMR, LC-mass spectrometry, and computational studies, which also optimized the final structure. The Cu^{2+} complexes were characterized using electronic and vibrational spectra, magnetic susceptibility, molar conductivity, a variable temperature magnetometer, and ESR spectroscopy. Cyclic voltammetry revealed electron transfer from Cu^{2+} to Cu^{+} within the complex. The in vitro tumour activity of the Cu^{2+} complexes and imine base were evaluated on the A431 cell line using the MTT assay. DFT studies validated the structural stability of the imine base. The antiferromagnetic behaviour observed at low temperatures suggests that these Cu^{2+} complexes could be useful in heavy magnetic materials. Due to their electron transfer properties, Cu^{2+} complexes also hold potential for use in electroplating systems and sensors. The complexes exhibited high efficacy on the cell line, aligning with clinical objectives. The Cu^{2+} complexes are represented as [MLR], where M is the metal, L is the imine base, and R = [C_6H_5COO] or R = [$C_6H_4COO(NH_2)$].

Keywords VSM, ESR, Invitro cytotoxicity, LC–MS, DFT studies, MEP mapping, Cyclic voltammetry

Complexes obtained from Schiff bases have provided insights for scientists into their flexibility in undergoing changes via reductions, eliminations, and additions[1]. These changes have led to the creation of numerous pharmacological[2–4] and bio-transition compounds[5]. According to recent studies, these complexes exhibit potential antimicrobial[6,7], antiviral[8,9], and photocatalytic[10] properties, and could potentially act as mimetic structures for enzyme models. Only limited synthetic practices have been described so far, including the

[1]PG and Research Department of Chemistry, Muthurangam Govt. Arts College, Tamil Nadu, Otteri, Vellore 632 002, India. [2]Department of Chemistry, Dr. M.G.R. Govt. Arts and Science College for Women, Tamil Nadu, Villupuram 605 401, India. [3]Department of Chemistry, Saveetha School of Engineering, Saveetha Institute of Medical and Technical Sciences (SIMATS), Saveetha University, Chennai 602 105, Tamil Nadu, India. [4]Department of Biochemistry, Dr. M. G. R. Chockalingam Arts College, Irumbedu 632317, Tamil Nadu, India. [5]Department of Botany and Microbiology, College of Science, King Saud University, PO Box-2455, Riyadh 11451, Saudi Arabia. [6]University Centre for Research and Development, Department of Civil Engineering, Chandigarh University, Mohali 140103, India. [7]Department of Biotechnology, PSGR Krishnammal College for Women, Peelamedu, Coimbatore 641004, India. [8]Department of Mechanical Engineering, Aditya University, Surampalem 533437, India. [9]School of Mechanical Engineering, Mettu University, Metu, Ethiopia. [10] Research Institute of IoT Cybersecurity, Department of Electronic Engineering, Research Institute of IoT Cyb National Ksohsiung University of Science and Technology, Kaohsiung, Taiwan. ✉email: senthil_geetha@rediffmail.com; geethakg0503@gmail.com; nasimhasan78@gmail.com

combination of amines and alcohols, dehydrogenation of primary amines, dimerization, and others. Due to the widespread availability of primary amines, the most common and efficient imines[11] have traditionally been obtained through the condensation of aldehydes and diamines. Our interest in the chelation process of imine ligands stems from the fact that the chelating moiety provides a unique labile complex that explains bonding behaviour[12,13]. The chelating sites in the imine base contribute to the geometrical stability of the complexes. The imine base has extensive applications in the pharmacological, clinical[14,15], and industrial fields. In bioinorganic chemistry, copper plays a significant role as a nutrient in respiration. Copper acts as a blood pigment in aquatic vertebrates, while in humans, it is found in bone marrow and the liver. Metalloenzymes containing Cu exhibit a variety of redox behaviors due to the presence of both lower and higher oxidation states, depending on ligand donors in the protein environment. As a result, active Cu ions participate in electron transfer and reversible oxygen (O_2) binding. The Cu(II) ion, the most common oxidation state of copper, is the most extensively studied transition metal. The magnetic properties depend on the species formed, whether mononuclear or polynuclear[16], and vary significantly from paramagnetic to antiferromagnetic to ferromagnetic behaviour[17]. Like other transition metal ions in the 3d series, Cu^{2+} complexes exhibit various geometries such as square planar[18], trigonal bipyramidal[19], and octahedral[20], with secondary valencies of four, five, and six, respectively.

Cancer research is a critical issue, with the development and advancement of effective clinical agents being a substantial priority. Modern advancements in technology and disease detection have expanded the possibilities for developing novel therapies, including targeted therapies[21,22]. This manuscript reviews the progress and challenges in the field and explores potential emerging methodologies. The imine base is a versatile group with significant pharmacological applications[23]. N,O-donor imine base-containing drugs have shown antiviral and anticancer activities by targeting specific proteins, pathways, or cells. Due to their broad therapeutic potential, N,O-donor imine base-containing drugs have become a key area of investigation in drug development. Recent cytotoxic studies focused in breast cancer cell line and lung cancer line. Due to the A431 cell line is widely utilized in skin cancer research due to its easy accessibility, epithelial shape, and ability to imitate the characteristics of epidermoid carcinoma[24–26]. This makes it a valuable tool for testing possible anti-cancer drugs and skin cancer-specific treatments and allows researchers to investigate the molecular mechanisms behind the growth, invasion, and metastasis of skin cancer.

We describe three novel compounds, including the imine base 2,6-bis((E)-(2-aminophenylimino)methyl)-4-methoxyphenol, in this article and provide molecular modeling studies using the DFT method. The synthesized Cu^{2+} complexes underwent various spectral analyses. The potential cytotoxic properties of the three compounds were evaluated.

Materials and methods

Materials and measurements

High-quality chemicals were used for the synthesis of the complexes, and they were used as received. 2,6-Diformyl-4-methoxyphenol was purchased from Sigma Aldrich, while benzoic acid, $CuSO_4{\cdot}5H_2O$, PABA, TBAB, o-phenylenediamine, perchloric acid, sodium hydroxide, sodium perchlorate, and C_2H_5OH were purchased from SD Fine Limited.

A German-made elemental analyzer, Vario EL, was used for the microanalysis of the imine base (HL) and its complexes. The molar conductivity of Cu^{2+} complexes were noted using an Elico conductometer (EQ-665, India). The λmax measurement of the imine base (HL) and Cu^{2+} complexes were verified by a UV–VIS Spectrophotometer-2202 (double beam), Systronics, India, within the range of 200–800 nm. The stretching and bending modes of the imine base (HL) and Cu^{2+} complexes were obtained using an IR-Affinity-I spectrometer, Shimadzu, Europe, by the KBr technique. The proton environment of the imine base (HL) was analyzed using the ^{1}H-NMR spectrum by a Bruker NMR (400 MHz model), Germany. LC–MS spectra of the imine base (HL) and Cu^{2+} complex was examined using a Waters—Xevo G2-Xs-QTof instrument model, Germany, which provided valuable data on the imine base (HL) and Cu^{2+} complex. An appropriate combination of basis sets and theoretical methods can provide a good balance between computational efficiency and accuracy in the field of computational quantum chemistry[27]. All theoretical calculations were performed without any geometric constraints for 2,6-bis((E)-(2-aminophenylimino)methyl)-4-methoxyphenol using the B3LYP energy functional[28–31] included in the Gaussian 09 W program suite[32]. The harmonic vibrational frequencies of the molecules were calculated through the DFT/B3LYP energy functional with the basis set, 6–311 + + G(d,p). Cu^{2+} complexes were examined using a VSM Lake Shore-7404 device model, USA, in the range of 10–250 K. Temperature variations modify and determine the magnetic nature of the material. ESR of Cu^{2+} complexes was recorded using an EMX X-BAND Bruker ESR model, Germany, at room temperature with DPPH as the internal standard. The CV of Cu^{2+} complexes were performed in dilute DMF solution using an HCH 5.01 600c electrochemical analyzer, Sinsil International, India, in an inert atmosphere using a three-electrode system: GCE (glassy carbon) as the working electrode, platinum wire as the auxiliary electrode, and SCE as the reference electrode. The supporting electrolyte TBAP was prepared and recrystallized using hot alcohol. There are different assay methodologies that identify the number of viable eukaryotic cells. The tetrazolium reduction method was used to detect viable cells. Since several tetrazolium reduction methods are available, HL, C-I, and C-II were tested for in vitro cytotoxicity using the MTT assay.

MTT assay screening method

Human epidermoid carcinoma cell line (A431) was obtained from National Centre for Cell Science (NCCS), Pune, India. Cancer cells were propagated in ninety-six well plates, approximately 3×10^5 cells per plate, and subjected to 24 h of incubation in an environment with 5% CO_2. After the incubation period in a CO_2 incubator, varying concentrations about (0, 10, 20, 30, 40, 50, 60, 70, 80, 90 and 100 µl) of the imine base and Cu^{2+} complexes were added to the A431 cell line for 48 h[33]. MTT reagent (10 µl) was added to each well and incubated for 4 h

at room temperature. Purple-stained formazan crystals appeared, which were dissolved in dimethyl sulphoxide (DMSO) (100 µl). The ninety-six well plate was analyzed at 570 nm using an ELISA plate reader, with optical density (OD) measured to determine cell viability based on the proportion of surviving cells. The percentage of cell viability was expressed as:

$$\text{Cell viability } (\%) = \text{ Absorbance of treated cells/Absorbance of control cells} \times 100$$

Acridine orange-ethidium bromide dual staining

The IC_{50} concentration of the imine base (HL) and Cu^{2+} complexes was tested against the control for 24 h by screening the proliferated A431 epidermal SCC cells in 6-well plates, which produced approximately 1×10^6 cells per well. Cells were washed with PBS and transferred to glass slides after incubation[34]. For 20 min, cells were treated with acridine orange-ethidium bromide (AOEB) (1 µl). The morphology of apoptotic cells was examined using a fluorescent microscope.

Synthesis of 2,6-bis((E)-(2-aminophenylimino)methyl)-4-methoxyphenol

The process of preparing 2,6-bis((E)-(2-aminophenylimino)methyl)-4-methoxyphenol (HL) involved the utilization of 2,6-diformyl-4-methoxyphenol and o-aminoaniline stoichiometrically, the ratio was 1:0.5 and magnetic stirrer was utilized to stir the components for three hours in ethanol, was portrayed in Fig. 1. TLC was used to monitor the progress of the reaction by using the eluent (hexane) and the transformation of color was spotted.

The carbonyl (R-CHO) compound (dial) treated with 1° amine (a diamine) engenders azomethine base (2,6-bis((E)-(2-aminophenylimino)methyl)-4-methoxyphenol) by dismissal of water molecule.

Preparation of Cu^{2+} carboxylates

Benzoic acid and PABA were used as primary source to create copper (II) carboxylates with sodium hydroxide and stirred for 30 min using stirrer. After forming composition, copper (II) sulphate pentahydrate was added, the mix was agitated for 120 min again was shown in Fig. 2. The stoichiometric ratio of sodiumhydroxide, primary source and $CuSO_4$ was used were in the ration of 2:2:1. Synthesized Cu (II) carboxylates were washed with water, ethanol and dried after being attained. The binuclear Cu^{2+} precursors obtained were used as primary source to formulate Cu (II) complexes.

Preparation of Cu^{2+}complexes ($Cu_2C_{28}H_{25}N_4O_{12}Cl_2$ and $Cu_2C_{28}H_{26}N_5O_{12}Cl_2$)

Binuclear Cu^{2+} complexes (C-I & C-II) were formed by stirring method. The 2,6-bis((E)-(2-aminophenylimino) methyl)-4-methoxyphenol (HL) was deprotonated, by stirring with NaOH for 30 min in ethanol. The deprotonated 2,6-bis((E)-(2-aminophenylimino)methyl)-4-methoxyphenol (HL) in ethanol were utilized to mix the sodium perchlorate, copper (II) benzoate, and copper (II) PAB for 3 h was displayed in Fig. 3. The binuclear Cu^{2+} complexes were synthesized by combining the following constituents NaOH, 2,6-bis((E)-(2-aminophenylimino) methyl)-4-methoxyphenol (HL), Cu^{2+} carboxylates and sodium perchlorate in stoichiometric quantity 1:1:1:2.

C-I: R = C_6H_5, C-II: R = $C_6H_4(NH_2)$.

2,6-bis((E)-(2-aminophenylimino)methyl)-4-methoxyphenol with NaOH, Cu^{2+} carboxylates and $NaClO_4$ were utilized to achieve the Cu^{2+} complexes.

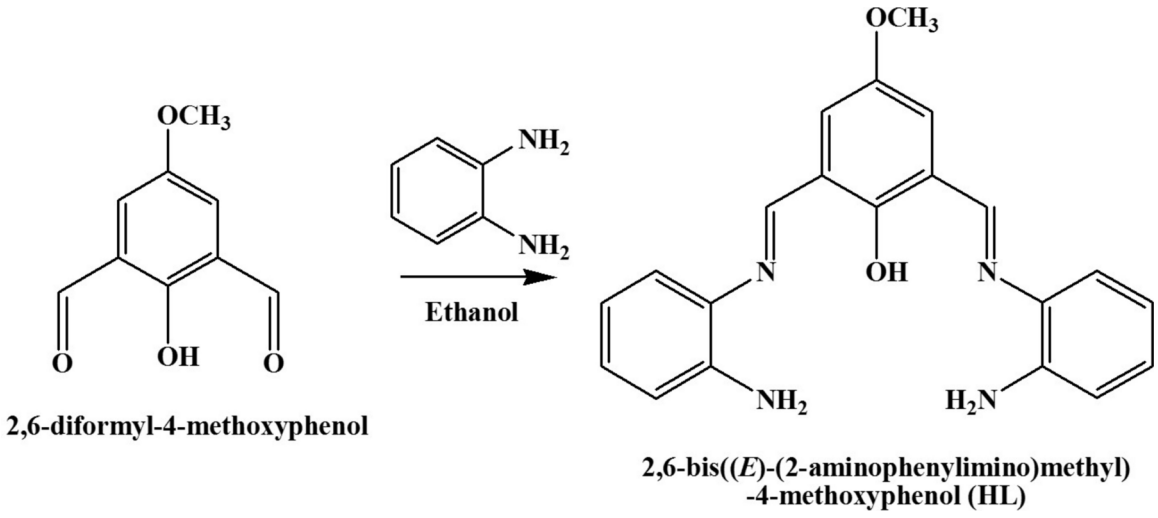

Fig. 1. Synthesis of 2,6-bis((E)-(2-aminophenylimino)methyl)-4-methoxyphenol (HL).

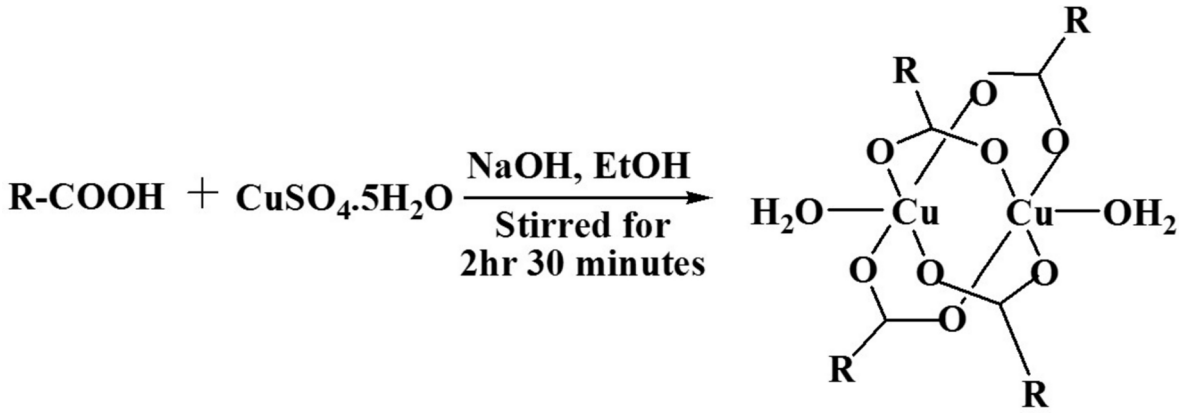

Fig. 2. Synthesis of Cu^{2+} carboxylates.

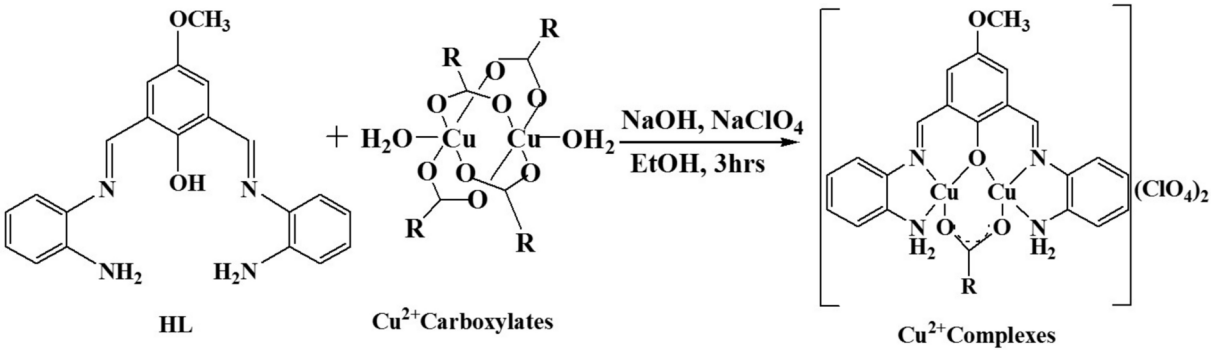

Fig. 3. Synthesis of Copper(II) complexes.

Compound	Empirical formula	Melting point (°C)	Molar conductance (Mho cm^2 mol^{-1})	Microstudy perceived (Cal.) (%)		
				C	N	H
HL	$C_{21}H_{20}N_4O_2$	107	–	74.69 (74.66)	14.47 (14.49)	6.36 (6.39)
C-I	$Cu_2C_{28}H_{25}N_4O_{12}Cl_2$	> 360	135	41.68 (41.65)	6.89 (6.94)	3.08 (3.12)
C-II	$Cu_2C_{28}H_{26}N_5O_{12}Cl_2$	> 360	146	40.92 (40.89)	8.58 (8.51)	3.14 (3.19)

Table 1. Imine base (HL) and its Cu^{2+} complexes.

Results and discussion

Molar conductivity measurements

DMF was utilized to measure the conductivity studies of Cu^{2+} complexes (C-I & C-II) and was compared to the reference 130–170 mho cm^2 mol^{-1}. Cu^{2+} complexes (C-I & C-II) revealed a 1:2 ionic environment[35], as demonstrated by conductivity values displayed in Table 1.

Electronic spectra

The 2,6-bis((E)-(2-aminophenylimino)methyl)-4-methoxyphenol (HL) and its Cu^{2+} complexes (C-I & C-II) at 10^{-3} M in DMF were analysed for electronic transition within λ_{max} 200–800 nm exhibits various electronic transition like π–π*, CT and d-d transitions, as displayed in Fig. 4. The 2,6-bis((E)-(2-aminophenylimino)methyl)-4-methoxyphenol (HL) showed a modest λ_{max} at 226 nm owed to the π–π* transition of an aromatic ring, C-I & C-II increased the λ_{max} to 239 nm and 242 nm after experienced a bathochromic shift[36] during complexation correspondingly. The azomethine group of 2,6-bis((E)-(2-aminophenylimino)methyl)-4-methoxyphenol (HL) contributed to the λ_{max} at 357 nm corresponding to the π–π* transition, subsequent complexation resulted in a red shift at λ_{max} of 364 nm & 367 nm for C-I & C-II, indicating the coordination of ligand with Cu^{2+} ion. The λ_{max} around 465 nm was attributed to charge transfer. Both C-I & C-II d-d transition showed weak wavelength of λ_{max} at 625 & 635 nm, respectively.

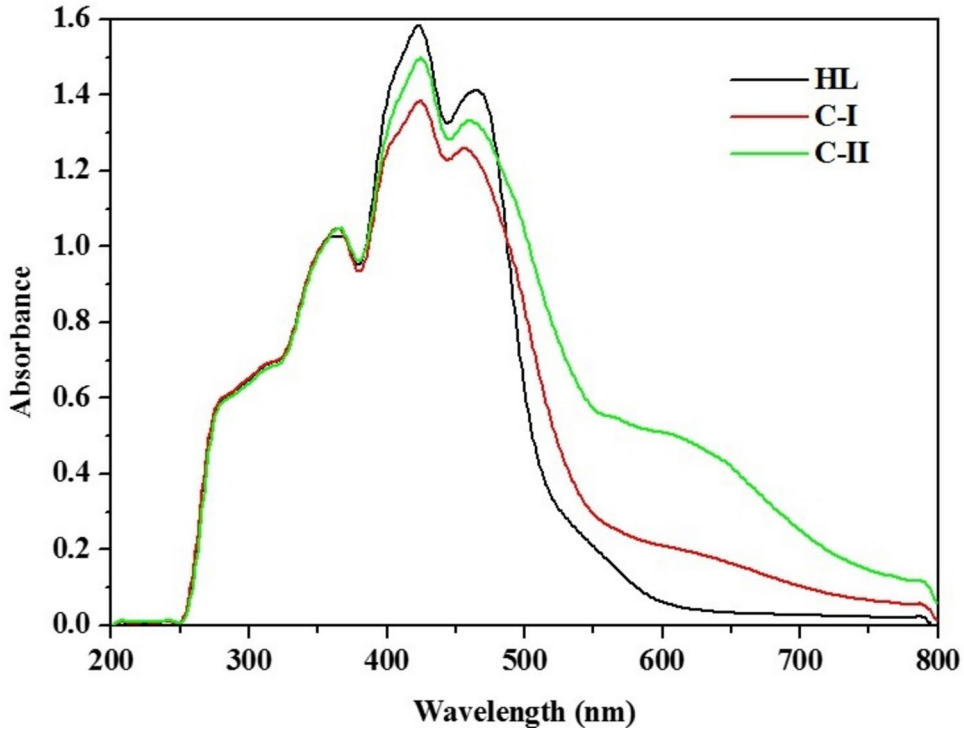

Fig. 4. UV–Visible spectra of HL, C-I and C-II.

Vibrational spectra

The binding mode between the complexes was examined by comparing the vibrational spectra of the complexes 2,6-bis((E)-(2-aminophenylimino)methyl)-4-methoxyphenol (HL) (Fig. 5). The substantial significant peaks of 2,6-bis((E)-(2-aminophenylimino)methyl)-4-methoxyphenol (HL) and its Cu^{2+} complexes were available in Table 2. 2,6-bis((E)-(2-aminophenylimino)methyl)-4-methoxyphenol (HL) exhibited an abrupt stretching frequency observed at 1633 cm^{-1}. The 2,6-bis((E)-(2-aminophenylimino)methyl)-4-methoxyphenol perceived an elongating frequency at 3255 cm^{-1}, consigned to (-C–OH) moiety. The (-C-O) group existence owed to the moderate peak at 1215 cm^{-1} in 2,6-bis((E)-(2-aminophenylimino)methyl)-4-methoxyphenol. 2,6-bis((E)-(2-aminophenylimino)methyl)-4-methoxyphenol has a distinct stretching frequency of 3423 cm^{-1} that indicates the amino group (–C–NH). An appreciable rise in the frequency value at 1265 cm^{-1} of -C-O group in vibrational spectra of C-I and C-II confirms the binding of Cu^{2+} ion with the oxygen atom of phenyl group through the proton expulsion. 2,6-bis((E)-(2-aminophenylimino)methyl)-4-methoxyphenol on complexing resulted in a lesser frequency of 15–20 cm^{-1} in stretching frequency at 1610 cm^{-1} appropriate for –HC = N group in the complexes[37]. Formation of the Cu^{2+} complexes was well supported through the peaks attained by resulting groups (Cu-carboxylate), (Cu–O), (Cu–N) and perchlorate ion in its outer sphere. The mounts attained around 1554 cm^{-1} and 1390 cm^{-1} are associated with asymmetric and symmetric stretching of (Cu-OCO) bond. The bidenticity of (-OCO) with complexes, was due to the difference between the symmetric and asymmetric carboxyl binding frequency was in the region of 164 cm^{-1}, relatively lower than the free carboxylate anion (195 cm^{-1})[38].

^{1}H-NMR of 2,6-bis((E)-(2-aminophenylimino)methyl)-4-methoxyphenol

^{1}H-NMR spectrum significantly envisaged the accurate environs of the relevant protons in the 2,6-bis((E)-(2-aminophenylimino)methyl)-4-methoxyphenol. Using TMS as a reference (internal), the ^{1}H-NMR spectrum of the 2,6-bis((E)-(2-aminophenylimino)methyl)-4-methoxyphenol was portrayed in Fig. 6 in DMSO-d_6 (solvent). The peaks (multiplet) at 6.5–7.7δ are attributed to methine protons of the benzenoid ring. The Chemical shift at 13.7δ is due to the proton of hydroxyl group (–OH)[39]. The azomethine group proton at 8.8δ exhibits an identical environment in 2,6-bis((E)-(2-aminophenylimino)methyl)-4-methoxyphenol. The peaks of multiplet at 4.4δ are attributed to the $–NH_2$ group protons. The methoxy group ($-CH_3$) protons are deshielded and show a singlet at 3.3δ.

Mass spectra

The 2,6-bis((E)-(2-aminophenylimino)methyl)-4-methoxyphenol (HL) and Cu^{2+} complex (C-I) mass spectra were represented in Figs. 7 and 8 respectively. The molecular ion peak assessment of HL and C-I supports the generation of 2,6-bis((E)-(2-aminophenylimino)methyl)-4-methoxyphenol and complex with dinuclearity[40]. The most intense peak, at 100% intense peak was the molecular ion peak of 2,6-bis((E)-(2-aminophenylimino) methyl)-4-methoxyphenol and Cu^{2+} complex i.e., m/z = 360 and m/z = 807, which was associated with the molecular weight (theoretical) of each, respectively. The value of m/z = 330 in 2,6-bis((E)-(2-aminophenylimino)

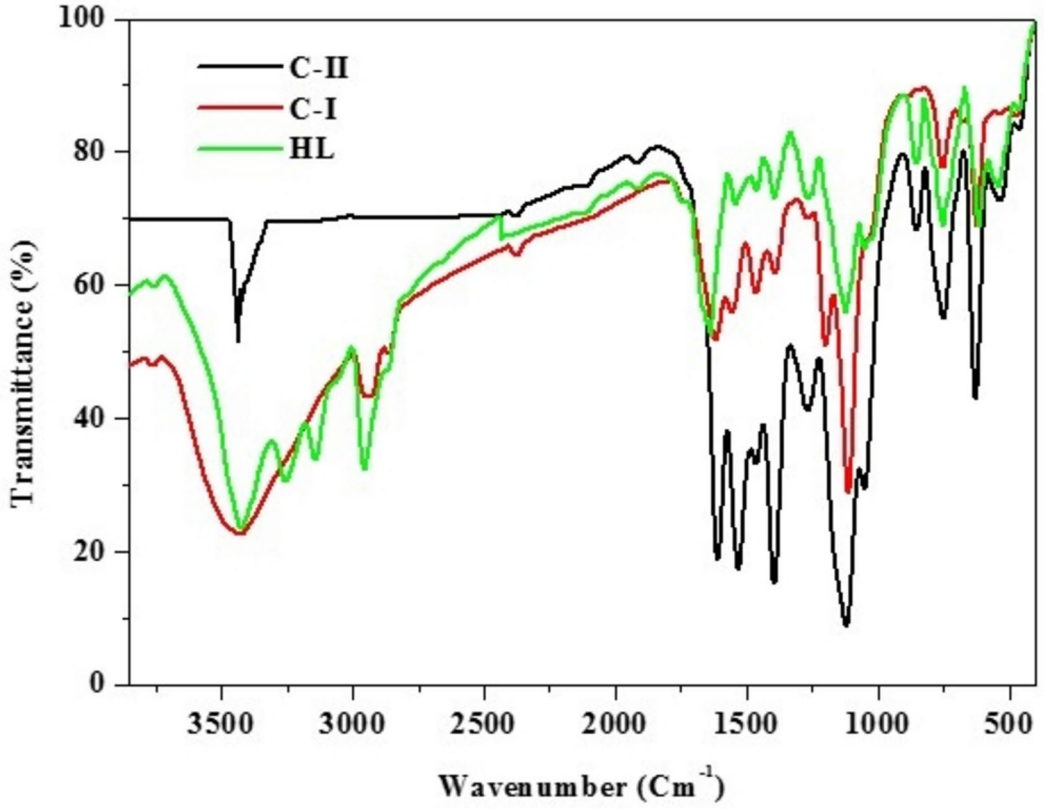

Fig. 5. Vibrational spectra of HL, C-I and C-II.

Moieties	HL (cm^{-1})	C-I (cm^{-1})	C-II (cm^{-1})
ν(C=N)	1633	1614	1610
ν(C–O)	1215	1261	1265
ν(–OH)	3255	–	–
ν(–NH)	3412	3423	3427
ν(–ClO_4)	–	1110	1120
ν(Cu–N)	–	534	532
ν(Cu–O)	–	472	461
ν(Cu–OCO)	–	1531, 1385	1554, 1390

Table 2. Stretching and bending modes of complexes and pentadentate ligand.

methyl)-4-methoxyphenol corresponds to the expulsion of the methoxy group. The removal of -NH_2 species from 2,6-bis((E)-(2-aminophenylimino)methyl)-4-methoxyphenol produces a fragment species at m/z = 315. A radical ion at m/z = 608 in Cu^{2+} (C-I) complex arises from the expulsion of the perchlorate ion associated with the outer sphere of the dinuclear complex.

Computational studies

HOMO–LUMO

Frontier molecular orbitals (FMO) were crucial in shaping the compounds optical and electrical properties. They have two types of energy levels (i) HOMO—molecular orbital that is highly occupied and, (ii) LUMO—molecular orbital that is lowest unoccupied. If an electron absorbs a photon, it is excited from a lower state energy to next higher state energy (ground level to excited state) likewise, in FMO, the electron transfers from HOMO to LUMO. The band energy gap of 2,6-bis((E)-(2-aminophenylimino)methyl)-4-methoxyphenol was calculated using B3LYP/6–311 + + G (d, p) level (Fig. 9a Frontier). Table 3 presents the energy of HOMO, LUMO and (HOMO–LUMO). Variation in energy within HOMO (– 5.2072 eV) and LUMO (– 2.0395 eV) was 3.1677 eV. A high band energy indicates that the amount of energy required to remove or add an electron from HOMO or LUMO, respectively, is high, making it a stable molecule. In a molecule, the FMO calculations provide the

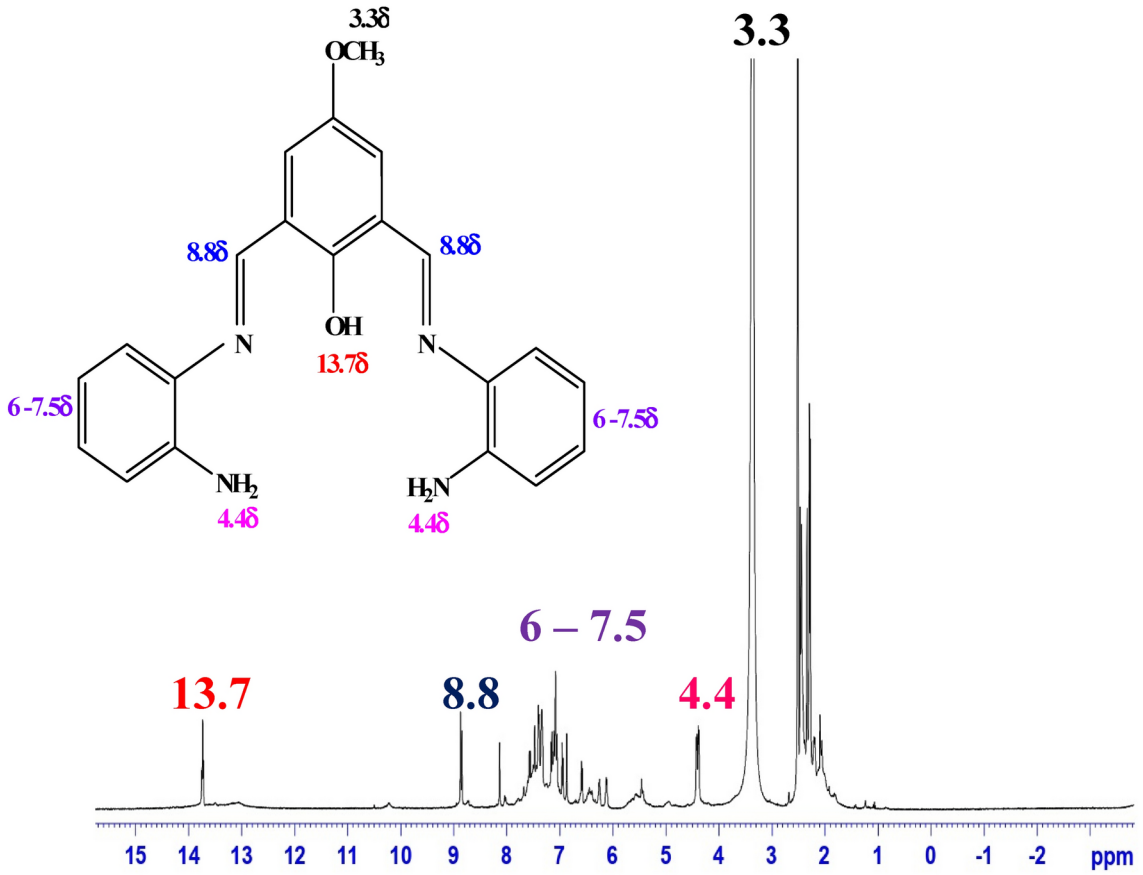

Fig. 6. ^{1}H-NMR of imine base (HL).

charges for all atoms, in which blue color represents negative charges and positive charges are given in red color. The charge distribution is attributed to the length of the bonds in the compound.

The frontier molecular orbital analysis of 2,6-bis((E)-(2-aminophenylimino)methyl)-4-methoxyphenol shows a high band energy gap indicates the higher stability (Fig. 9a) and this inference is further confirmed by the values obtained for the global reactivity parameters like (i) Ionization energy (IE) (ii) Electron gain enthalpy (EA) (iii) Electro inclination (χ), (iv) Smoothness (S), hardness (η) and potential (μ) of the Chemical and (v) Electrophilicity index (ω) depicted in Fig. 9b. The pictorial representation of the relation between the parameters with the stability of 2,6-bis((E)-(2-aminophenylimino)methyl)-4-methoxyphenol is depicted in Fig. 9c. The parameters determined using the following relation[41,42] (i) Gibbs Potential = 1/2 ($E_{LUMO} + E_{HOMO}$), (ii) Electro inclination = − 1/2 ($E_{LUMO} + E_{HOMO}$), (iii) Compound hardness = 1/2 ($E_{LUMO} - E_{HOMO}$), (iv) Electrophilicity index = μ 2/2η, (v) Chemical Softness = 1/η.

Molecular electrostatic potential (MEP) surface

The electrostatic properties in the molecules were extensively studied by the Molecular electrostatic potential (MEP), which enables the measurement of the whole charge dissemination and correlates it with molecular properties such as reactivity, dipole moment, partial charge and electro-negativity (molecular properties). It generates a visual representation of distribution of electron charges that renders to examine the molecules properties and behaviour. The MEP of the surface depicts the charge, shape, size, and density, which indicates the reactive sites in the molecules.

The differences in electrostatic potential values in molecules surface were visualized in various color. Electronegative potential regions were represented in red, while electropositive potential regions were shown in blue, and green color indicated the zero potential region. The potential followed the trend: red > orange > yellow > green > blue. Gaussian software (Gauss view) was applied to map the electrostatic potential of 2,6-bis((E)-(2-aminophenylimino)methyl)-4-methoxyphenol by applying B3LYP/6–311 + + G (d, p) energy functional (Fig. 10). Charge distribution in the molecule was observed through the generated colors, which also indicated the molecules active sites and bonding sites[43].

According to MEP map, the region around the hydrogen atoms in the aryl and methyl group shows a high positive potential (electron poor region) depicted in blue color, which is the reactive moiety. Due to the inductive effect and the presence of a higher electron cloud, the oxygen (methoxy and phenol group) and nitrogen atoms (amine group) exhibits vast negative potential shows red color, because of its binding capacity. The existence of numerous color in MEP map range from − 8.539e−2 and 8.539e−2 for 2,6-bis((E)-(2-aminophenylimino)

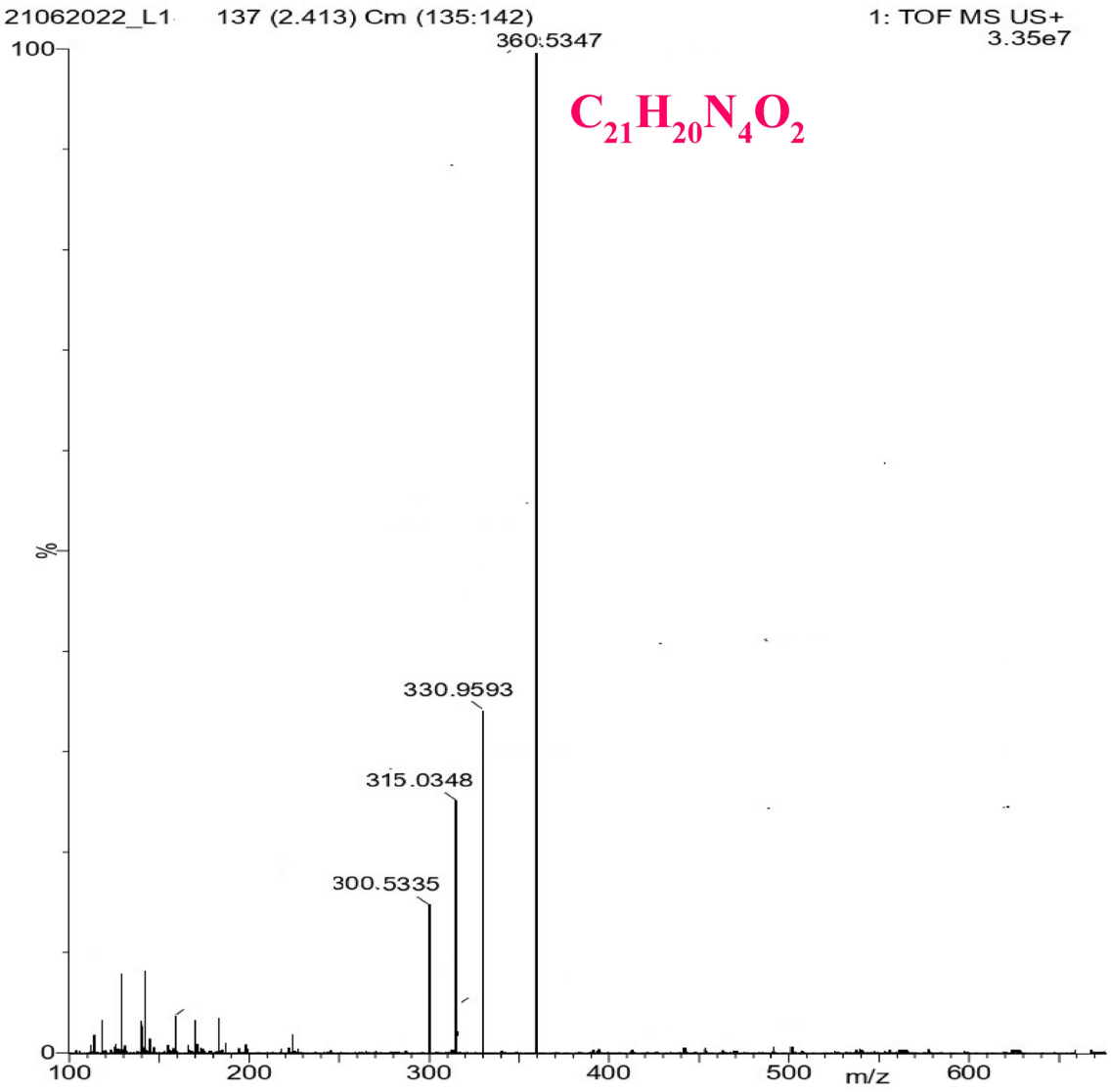

Fig. 7. Mass spectrum of imine base (HL).

methyl)-4-methoxyphenol, indicates the atoms experiencing strong repulsion are represented in red, while atoms with strong attraction are shown in blue. Atomic charges affect the electronic assembly, dipole moment, and polar nature of molecules.

Mulliken population analysis

In quantum chemical computations, the Mulliken nuclear charge distribution is widely utilized to demonstrate the magnetic, electronic and vibrational properties of molecular assemblies. This is because atomic charges impact molecular properties such as electronic structure, structural dipole moment and structural polarizability[44]. In addition, the atom charge of a molecular system offers a comprehensive depiction of charge transfer, electrophilic and nucleophilic reactions, atomic charge movement, and electrostatic potential overlays. Table 4 displays the calculation of the Mulliken charge dissemination of HL via B3LYP/6-311 + + G(d,p). Visualizing it in graphical form, as shown in Fig. 11, is a better approach.

The atomic charges of carbon, nitrogen and oxygen are given in Table 4. The nitrogen atom (1N, and 26N) of the free amino group has maximum negative charge of – 0.4096e, and – 0.4040e, respectively. Likewise, nitrogen atoms (19N, and 8N) which are attached to carbon atoms have a slight positive charge of 0. 1469 and 0. 1617 respectively.

There are two oxygen atoms present in the molecule, Oxygen of the hydroxyl group (–OH) (27O) has low negative value (-0.0520e) and oxygen of the methoxy group (16O) has a low negative value of – 0.1538e, it may be because the phenyl group bonded through hydroxyl oxygen perform an electron withdrawing and methyl species attached to 16O act as electron donating group[45].

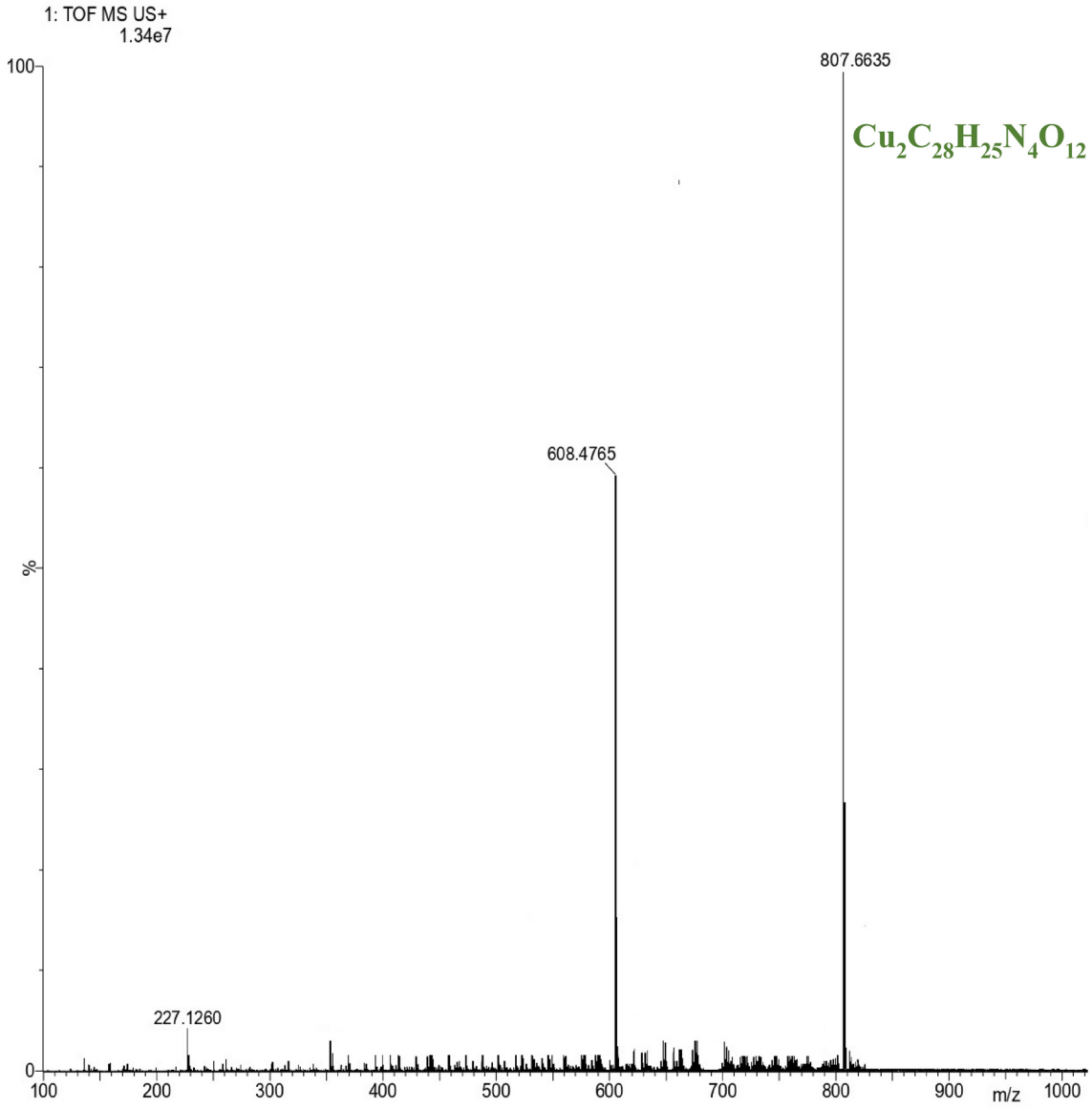

Fig. 8. Mass spectrum of C-I.

Some of the carbon atoms have negative charges, particularly C14 (− 0.9181e), and C17 (− 0.3619e) attached to 16O, and 11C (− 0.5371e) attached to 27O has maximum negative charges. This result indicates a strong correlation with MEP surfaces, as all hydrogen atoms have positive charges.

Magnetic susceptibility

Magnetic susceptibility of Cu^{2+} complexes was attained using Gouy balance at room temperature. The assessment of Cu^{2+} complexes involved evaluating both the magnetic susceptibility and the actual magnetic moments (μ_{eff}). The assessed magnetic moment (μ_{eff}) by Gouy method of Cu^{2+} complexes were 1.70 and 1.69 BM and it was while minimum related to the spin value of Cu^{2+} (1.73 BM). μ_{eff} values validated that C-I and C-II represent an unpaired electron.

VSM analysis

According to the basics, magnetic materials exhibit either diamagnetism or paramagnetism when diluted, while increasing concentrations can show ferro-, antiferro-, or ferrimagnetism. Using Gouy's method, an unpaired electron was found in the complexes at ordinary thermal conditions. To ascertain the magnetic properties at varying temperatures, VSM (Vibrating Sample Magnetometry) proves to be a useful tool. The Cu^{2+} complexes were examined by VSM in the temperature range of 10–250 K. Magnetism was measured in emu/g. The magnetic nature of the complexes was determined by plotting χmT against T, and the results are illustrated in Fig. 12.

For the Cu^{2+} complex, the magnetic susceptibility was observed to be 0.0048 cm^3 $Kmol^{-1}$ and 0.0049 cm^3 $Kmol^{-1}$ at 250 K, and the effective magnetic moment was calculated as 1.70 BM and 1.71 BM, respectively. As the

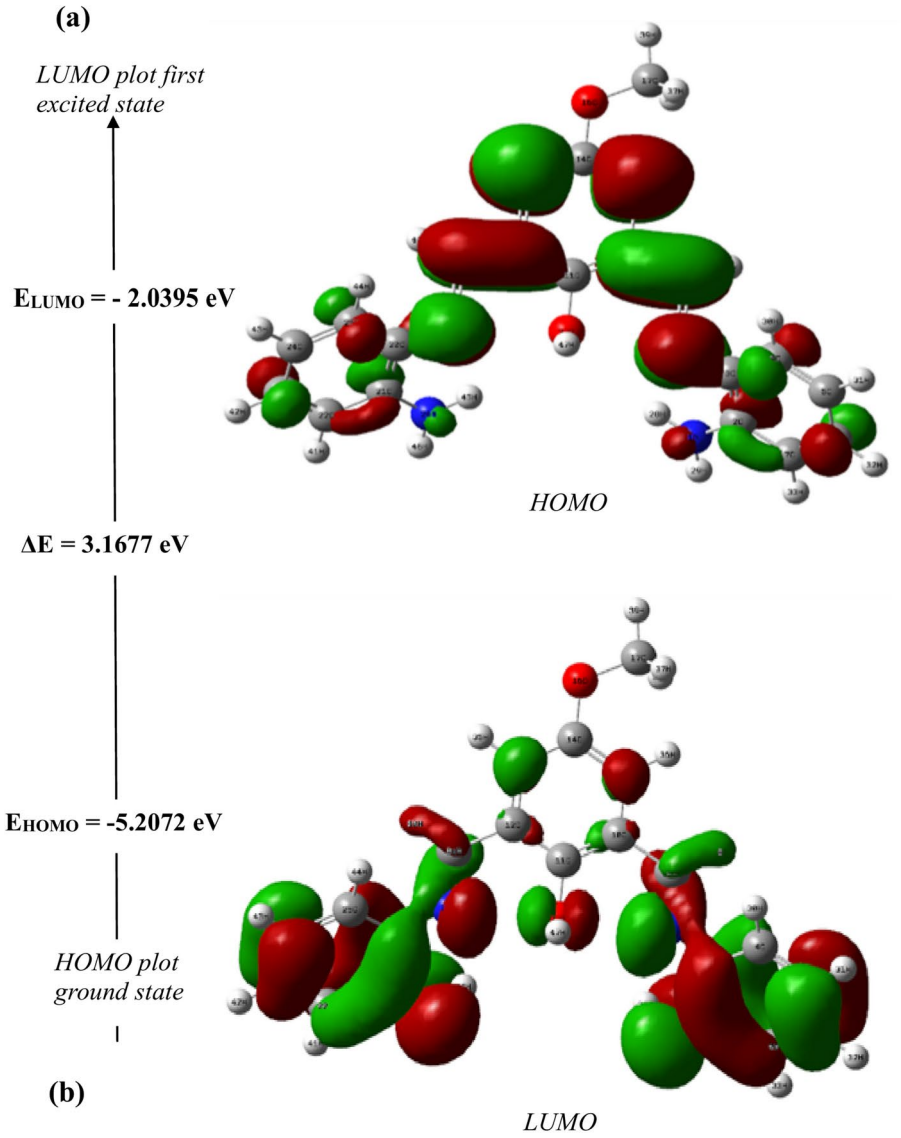

Parameter	Values B3LYP/6-311++G(d,p)
HOMO (eV)	-5.2072
LUMO (eV)	-2.0395
Ionization potential (IP)	5.2072
Electron affinity (EA)	2.0395
Energy gap(eV)	3.1677
Electronegativity (χ)	3.6234
Chemical potential (μ)	-3.6234
Chemical hardness (η)	1.5839
Chemical softness (S)	0.3157
Electrophilicity index (ω)	4.1445

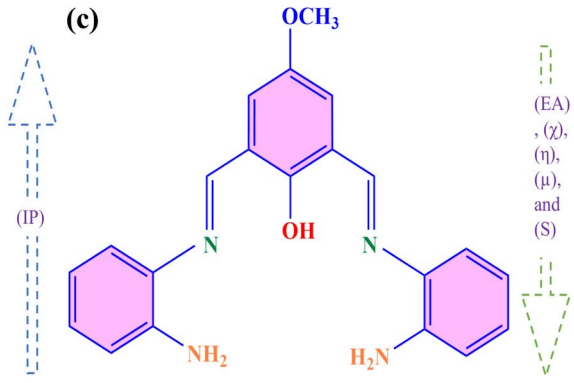

Fig. 9. (**a**–**c**) Frontier molecular orbital of imine base (HL).

temperature decreased, the susceptibility progressively diminished. The susceptibility showed a gradual decrease at regular intervals down to 25 K, followed by a significant decline at 10 K, suggesting an antiferromagnetic nature at lower temperatures. The super exchange interaction between the Cu-Cu moieties was facilitated by the bridged (–COO–) ion, as indicated by the magnetic behavior of the complexes (C-I and C-II)[46,47].

Parameters (eV)	B3LYP/6 31G (d,p)
HOMO energy	− 5.2072 eV
LUMO energy	− 2.0395 eV
HOMO–LUMO energy	3.1677 eV

Table 3. HOMO–LUMO energy and energy gap of 2,6-bis((E) (2aminophenylimino) methyl)-4-methoxyphenol.

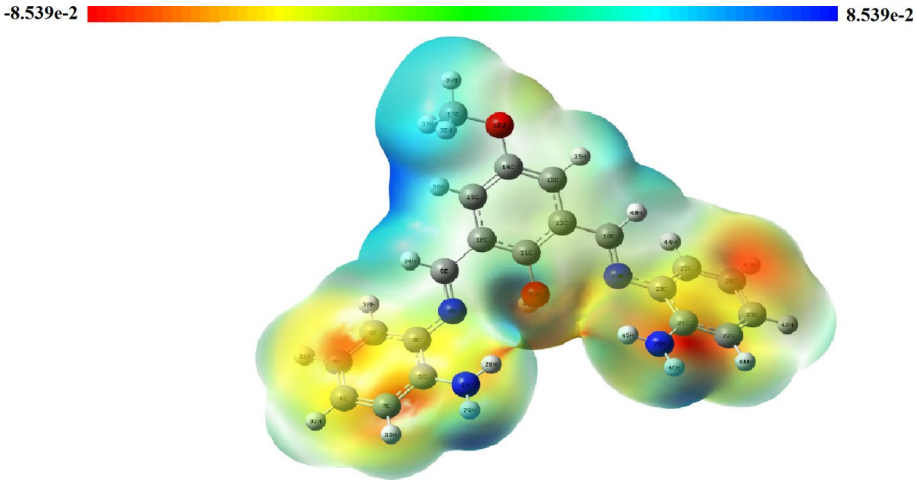

Fig. 10. MEP of imine base (HL).

Atoms	Charges	Atoms	Charges	Atoms	Charges
1 N	− 0.4096	17 C	− 0.3619	33 H	0.1388
2 C	0.1572	18 C	0.0901	34 H	0.1316
3 C	− 0.0810	19 N	0.1469	35 H	0.1865
4 C	0.0010	20 C	− 0.2238	36 H	0.1366
5 C	− 0.2396	21 C	0.2350	37 H	0.1533
6 C	− 0.3356	22 C	− 0.2136	38 H	0.1556
7 C	− 0.2020	23 C	− 0.3629	39 H	0.1922
8 N	0.1617	24 C	− 0.2302	40 H	0.1321
9 C	− 0.1319	25 C	0.0035	41 H	0.1380
10 C	0.8076	26 N	− 0.4040	42 H	0.1439
11 C	− 0.5371	27 O	− 0.0520	43 H	0.1609
12 C	0.8587	28 H	0.2855	44 H	0.1375
13 C	− 1.3013	29 H	0.2662	45 H	0.3039
14 C	− 0.9181	30 H	0.1352	46 H	0.2636
15 C	0.0362	31 H	0.1602	47 H	0.2960
16 O	− 0.1538	32 H	0.1433		

Table 4. Atomic charge of imine base (HL).

ESR spectra

An axial symmetry was observed when the Cu^{2+} complexes were subjected to ESR at 30 °C. DPPH act as standard ($g_e = 2.003$). Several g factors and G values for the Cu^{2+} complexes were enumerated in Table 5 and displayed in (Fig. 13) relatively. The innumerable g parameters of the Cu^{2+} complexes reveal the subsequent fashion $g^{||} > g\perp > g_e$, that designated the existence of $dx^2\text{-}y^2$ in the most stable state (ground) and the single electron reside in it. Hence the Cu^{2+} complexes recommended square planar form[48]. The covalent nature of C-I and C-II among the M-L rendering by the lesser $g^{||}$ value of 2.3, reflecting the metal ligand interaction.

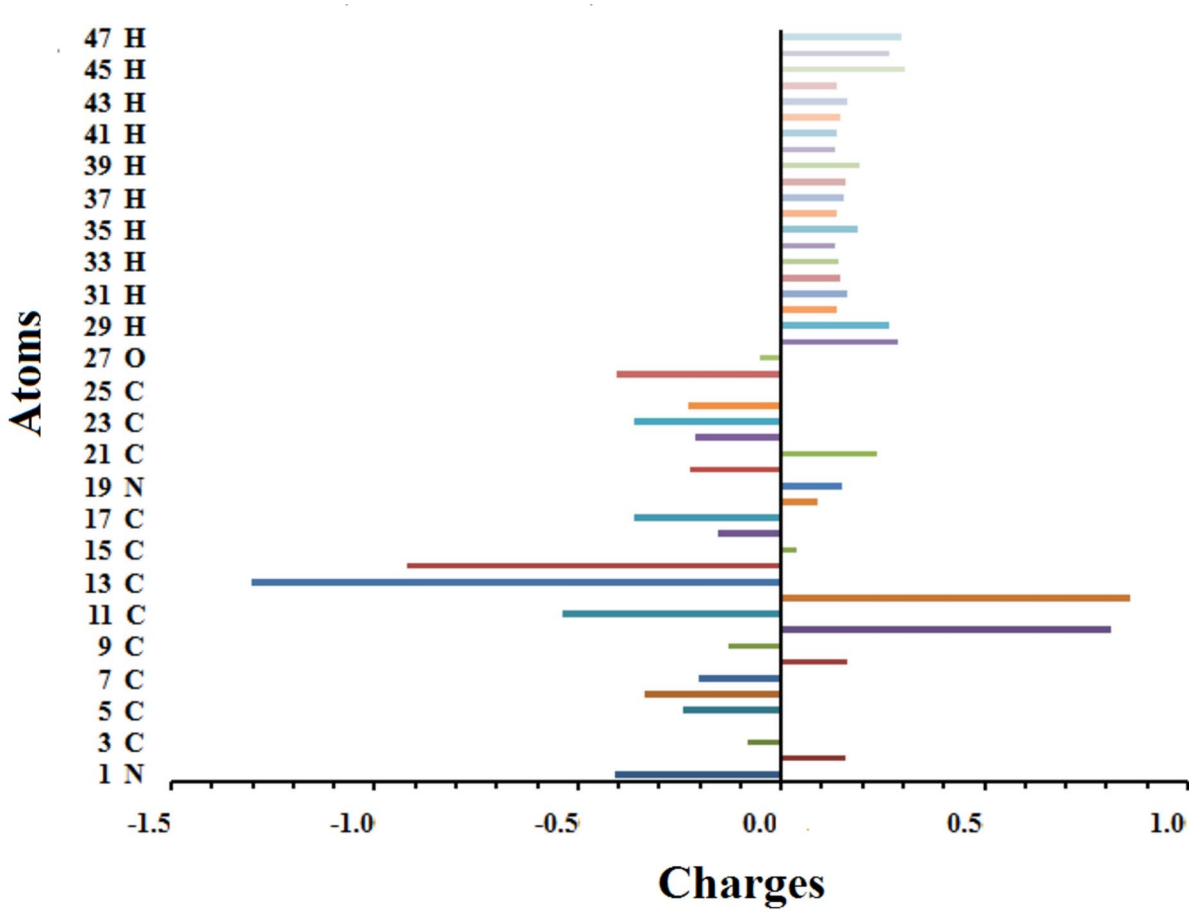

Fig. 11. Mulliken Charge Plot of HL.

Cyclic voltammetry

To verify the natural redox conditions, we investigated Cu^{2+} complexes (C-I and C-II) in DMF by cyclic voltammetry scanning (CV). Tetrabutylammoniumperchlorate utilized as supporting electrolyte. To maintain the inert atmosphere, N_2 gas was surpassed continually. Table 6 exemplified the redox data attained, and Fig. 14 represents the CV of C-I & C-II. The voltammogram found two electron removal quasireversible peaks for the Cu^{2+} complexes, respectively. The first quasireversible reduction potential meant for the Cu^{2+} complexes was noticed as − 0.7009 V and − 0.8998 V, correspondingly. Analogously, the second quasireversible reduction was noted as − 1.1199 V and − 0.5795 V respectively. The electron transport for the first quasireversible peak was noted to be one[49] ($n \approx 0.92$) accompanied via each quasireversible peak associated to $1e^-$ transfer will in the arrangement of $Cu^{II}Cu^{II}/Cu^{II}Cu^{I}$ redox couple. Divergent valent $Cu^{II}Cu^{II}/Cu^{I}Cu^{I}$ species were resembling the establishment of the second quasireversible wave. The voltammogram displayed, a stepwise redox progression in the Cu^{2+} complexes which signified as:

$$Cu^{II}Cu^{II} \rightleftharpoons Cu^{I}Cu^{II} \rightleftharpoons Cu^{I}Cu^{I}$$

Anticancer activity

The 2,6-bis((E)-(2-aminophenylimino)methyl)-4-methoxyphenol (HL) and its Cu^{2+} complexes (C-I and C-II) were screened by A431 cell line for *invitro* anticancer studies using MTT evaluation approach. The half disintegration lifeless tumour cells were illustrated as $IC_{50} \pm$ S.E.M. The cells' cytotoxic effects were exposed to the HL and Cu^{2+} complexes through a concentration-reliant means. Disintegration was not attained in the cells before exposure to complexes and the ligand. The 2,6-bis((E)-(2-aminophenylimino)methyl)-4-methoxyphenol and Cu^{2+} complexes with the strength among 0–100 µg/ml was investigated towards A431 cell, the viability of cell diminished on escalating the strength of the investigating compounds. The 2,6-bis((E)-(2-aminophenylimino) methyl)-4-methoxyphenol (HL) had the half disintegration cell value at 53 µg/ml, after coordinating with Cu. The attained Cu^{2+} complexes established higher influence than the non-coordinated 2,6-bis((E)-(2-aminophenylimino)methyl)-4-methoxyphenol as presented evidently in Fig. 15. The Cu^{2+} complexes exhibit IC_{50} for C-I at 35 µg/ml, and the IC_{50} for C-II at 24 µg/ml, relatively[50]. It was validated that Cu^{2+} complex C-II has a higher potency on A431 cell line because of an electron-liberating group comparable with Cu^{2+} complex C-I[51]. Independent 2,6-bis((E)-(2-aminophenylimino)methyl)-4-methoxyphenol (HL), the IC_{50} was greater than the

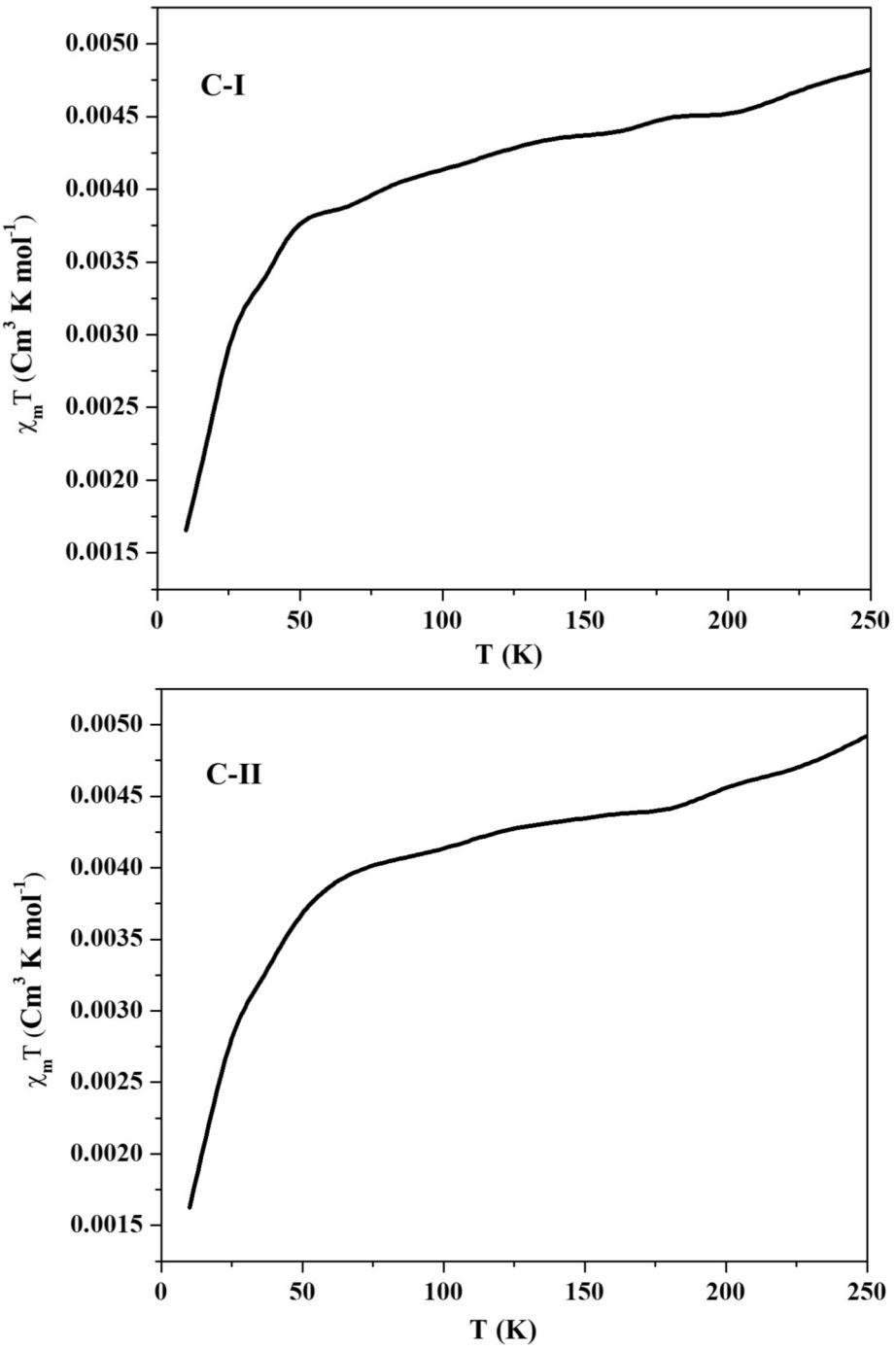

Fig. 12. The plot of $\chi_m T$ vs T for complex C-I and C-II.

Compound	$g^{\|\|}$	$g^{\perp}$	g_{iso}	G
C-I	2.0807	2.0299	–	2.6858
C-II	2.0930	2.0303	–	3.1049

Table 5. g parameters and G-value of C-I and C-II.

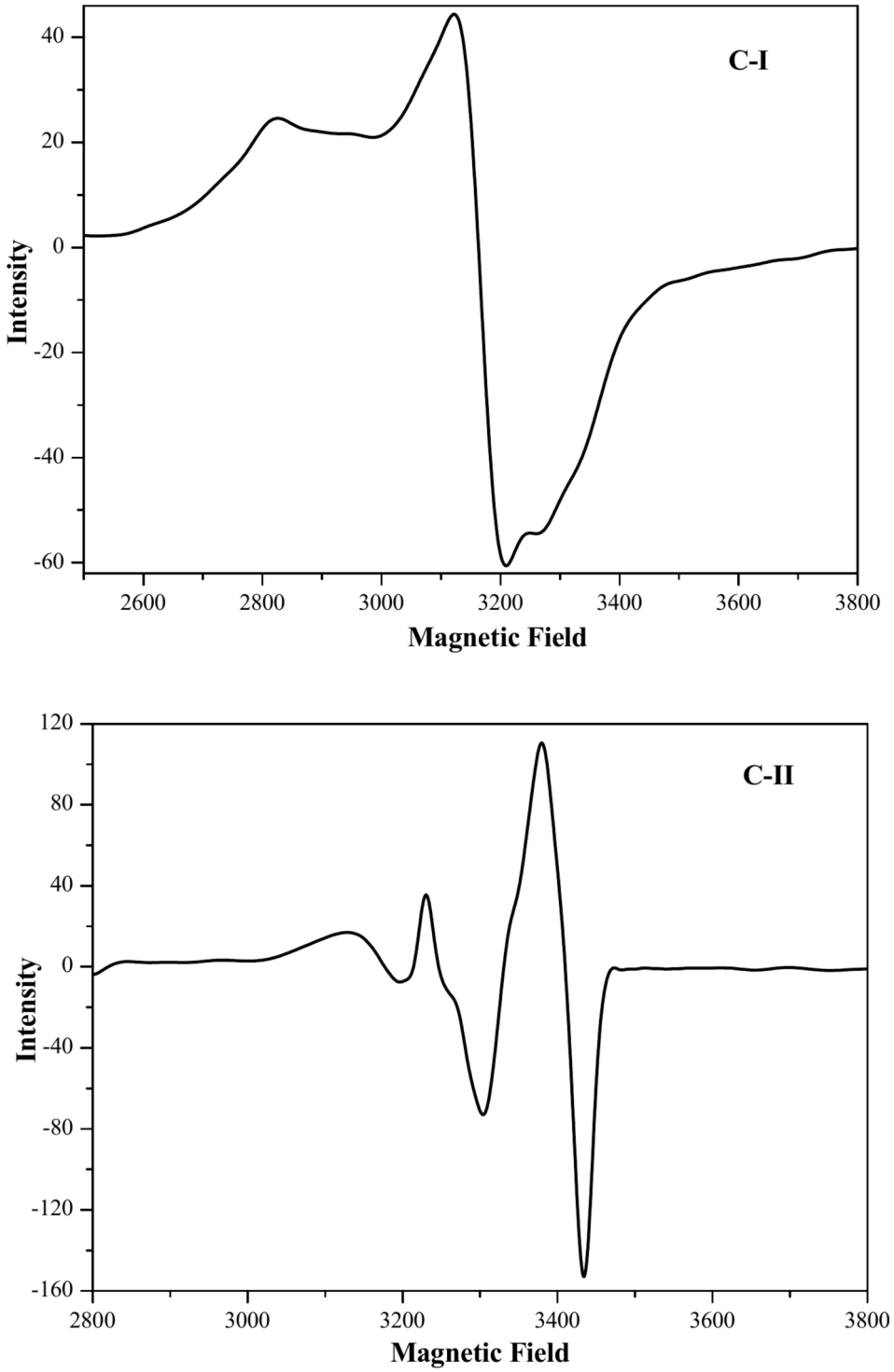

Fig. 13. ESR spectrum of complex C-I and C-II.

Complex	E^1_{PC} (V)	E^1_{Pa} (V)	E^2_{PC} (V)	E^2_{Pa} (V)
C-I	− 0.7009	− 0.8268	− 1.1199	0.8478
C-II	− 0.8998	− 0.7176	− 0.5795	0.9124

Table 6. Electrochemical data of Cu^{2+} complexes.

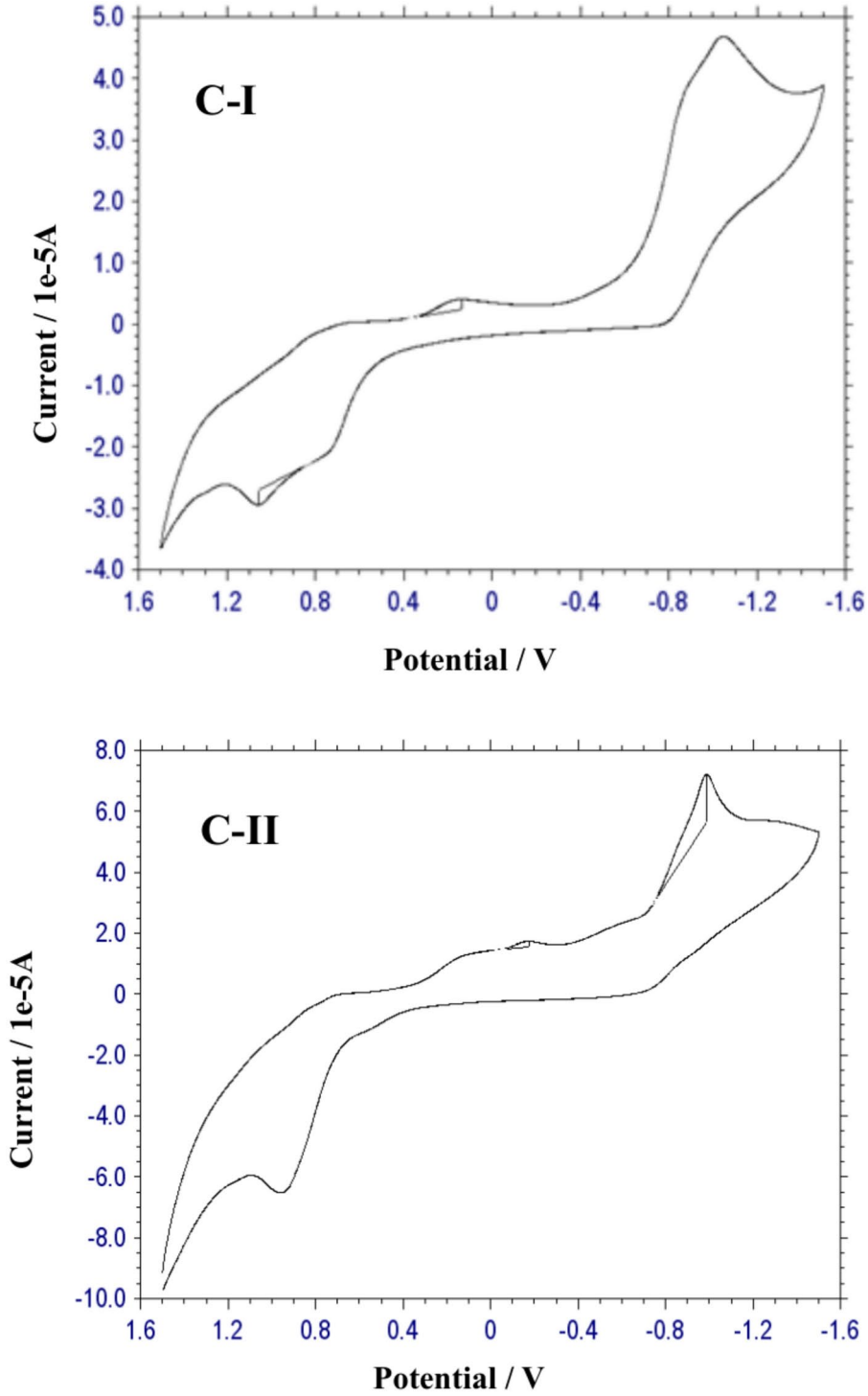

Fig. 14. Cyclic voltammogram of C-I and C-II.

complexes, represents that the independent 2,6-bis((E)-(2-aminophenylimino)methyl)-4-methoxyphenol (HL) has reduced potency on the cell line than complexes.

Staining by acridine orange-ethidium bromide

2,6-bis((E)-(2-aminophenylimino)methyl)-4-methoxyphenol (HL) and Cu^{2+} complexes were analysed with the help of fluorescence microscopy. Green, yellow, and reddish or orange staining were used to represent sustainable cells, initial affected cells, and deceased cells[52]. The control consisted of green stained cells that consistently had a bulky nucleus. Based on the available data, it was concluded that the compounds produced caused significant apoptosis in cancer cells, which demonstrated membrane blebbing and chromatin compression. Acridine orange/

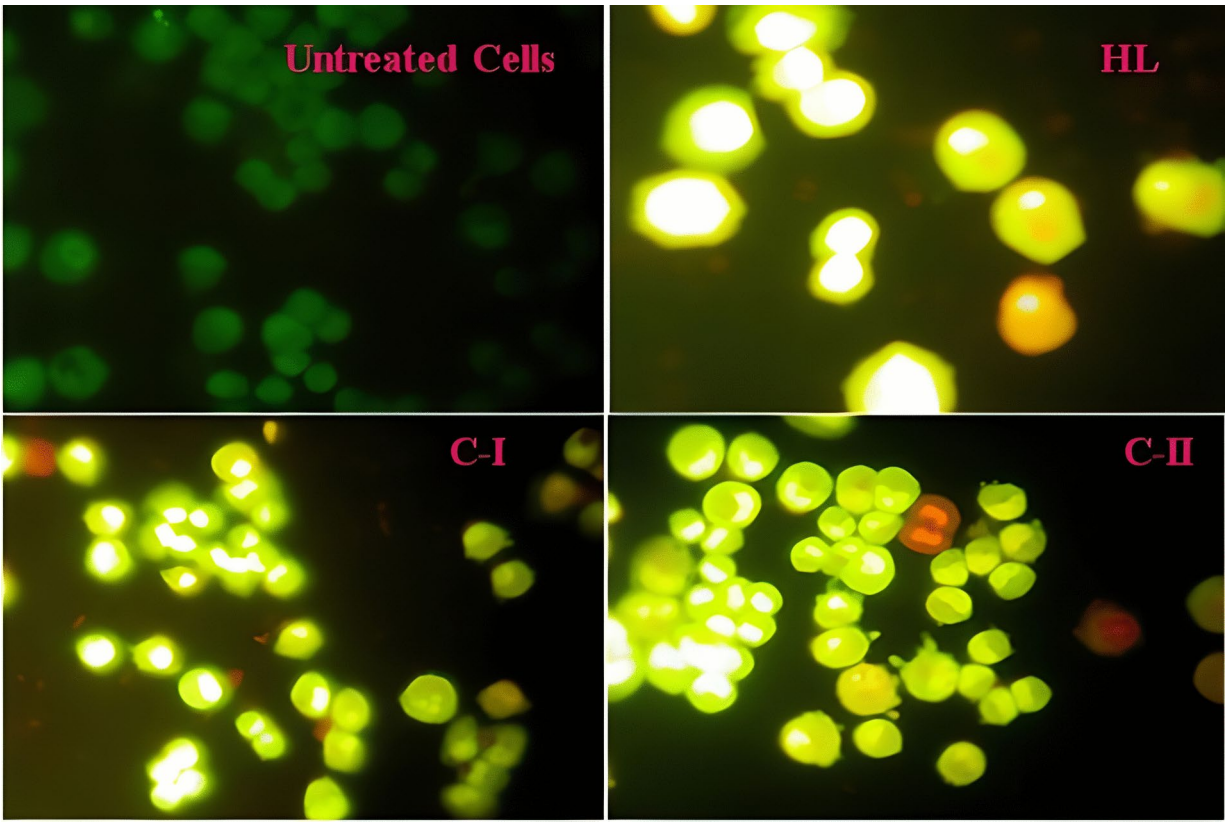

Fig. 15. Cytotoxic fluorescence image of imine base (HL) and complexes C-I and C-II.

ethidium bromide, which is capable of penetrating into apoptotic cells, was used to verify the effectiveness of 2,6-bis((E)-(2-aminophenylimino)methyl)-4-methoxyphenol, C-I and C-II in inducing apoptosis in A431 cells, which resist chemotherapy in A431 cells. The fluorescence picture and graphical illustration of cytotoxicity of 2,6-bis((E)-(2-aminophenylimino)methyl)-4-methoxyphenol and (C-I and C-II) were provided in Figs. 15 and 16, correspondingly[53].

Conclusion

2,6-bis((E)-(2-aminophenylimino)methyl)-4-methoxyphenol (HL) and its Cu^{2+} complexes (C-I and C-II) were prepared successfully. From the basic examination and mass data the formula of 2,6-bis((E)-(2-aminophenylimino)methyl)-4-methoxyphenol (HL) and Cu^{2+} complexes was determined, and the formation of 2,6-bis((E)-(2-aminophenylimino)methyl)-4-methoxyphenol was evidently proved by proton-NMR spectrum. By obtaining the optimized structure from theoretical studies, we can gain more insight into the arrangement of 2,6,-bis((E)-(2-aminophenylimino)methyl)-4-methoxyphenol (HL). The molar conductivity of Cu^{2+} complexes obtained confirms 1:2 ionic nature. The UV–VIS and vibrational spectra depicted the functional moieties of 2,6-bis((E)-(2-aminophenylimino)methyl)-4-methoxyphenol and Cu^{2+} complexes. Specifically, the vibrational data explained the binding mode of the 2,6-bis((E)-(2-aminophenylimino)methyl)-4-methoxyphenol and the linking of the carboxylate group in complexes. Different g parameters, symmetry belongings and nature of environs were predicted from ESR of Cu^{2+} complexes. $g^{||}$ and $g^{\perp}$, were used to calculate G. The dx^2-y^2 orbital is where the single electron is located, and the Cu^{2+} complexes have a square planar shape. Cu^{2+} complexes display an antiferromagnetic environment during their magnetic behavior. The carboxyl moiety linking the Cu^{2+} ions in the Cu^{2+} complexes led to a strong exchange interaction between them, which caused changes in their shape. Cytotoxicity of Cu^{2+} complexes induced to be further potent compare with free 2,6-bis((E)-(2-aminophenylimino)methyl)-4-methoxyphenol. The Cu^{2+} complex (C-II) was highly effective than (C-I) due to the reason of electron liberating group. From an application perspective, the comparison appears to be highly effective. The structures can be determined using available data for 2,6-bis((E)-(2-aminophenylimino)methyl)-4-methoxyphenol and Cu^{2+} complexes C-I and C-II were recommended as follows in Fig. 17.

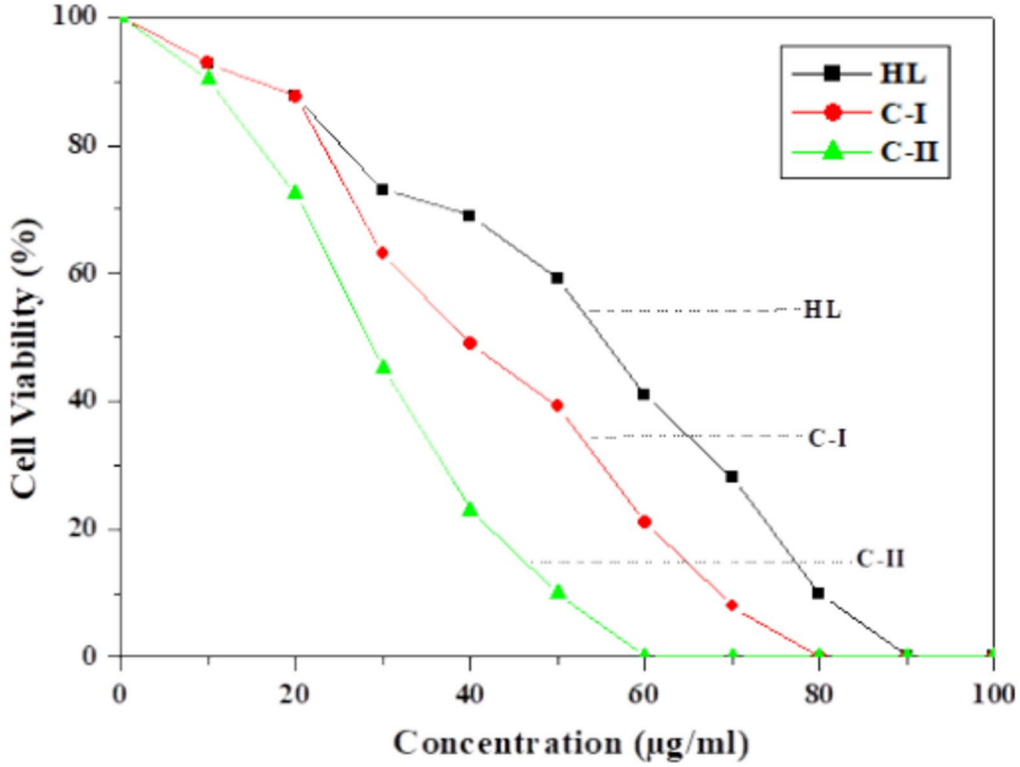

Fig. 16. Graphical representation of cytotoxicity of HL, C-I and C-II.

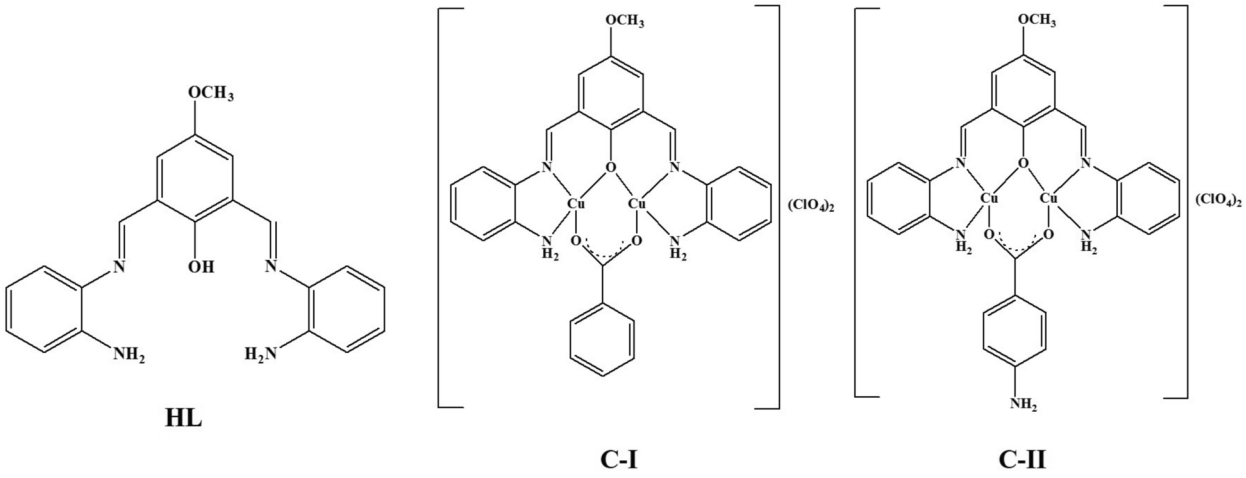

Fig. 17. Structure of HL, C-I and C-II.

Data availability

The datasets used and/or analyzed during the current study are available from the corresponding author upon reasonable request.

Received: 9 August 2024; Accepted: 5 February 2025
Published online: 26 February 2025

References

1. Arulmozhi, S. et al. Chemical, pharmacological, and theoretical aspects of some transition metal(II) complexes derived from pyrrole Azine schiff base. *ACS Omega* **8**, 34458–34470. https://doi.org/10.1021/acsomega.3c02860 (2023).

2. Musthafa, M. et al. Synthesis, characterization, and biological evaluation of Bis(Aroyl Thiourea) derivatives: Insights into their potential applications through DFT analysis. *Polycyclic Aromat. Compd.* **1**, 1–16. https://doi.org/10.1080/10406638.2023.2270115 (2023).
3. Al-Riyahee, A. A., Hadadd, H. H. & Jaaz, B. H. Novel Nickel (II), Copper (II) and Cobalt (II) complexes of Schiff bases A, D and E: preparation, identification, analytical and electrochemical survey. *Orient. J. Chem.* **34**, 2927–2941. https://doi.org/10.13005/ojc/340632 (2018).
4. Natarajan, A., Thangamani, R., Prabakarakrishnan, R., Ramanan, A. A. & Jayavelu, A. Investigation on potential efficacy of methanol extract of *Lawsonia inermis* L. against carbon tetrachloride induced hepatotoxicity in Wistar Albino rats. *Int. J. Pharm. Sci. Rev. Res.* **70**(1), 68–74. https://doi.org/10.47583/ijpsrr.2021.v70i01.009 (2021).
5. Prabakarakrishnan, R., Manoranjitham, S. & Geetha, K. Synthesis of copper (II) complexes using pentadentate Schiff base ligand by eco friendly solventless method and its antimicrobial activities. *World J. Pharm. Res.* **3**(9), 1286–1299 (2014).
6. Prabakarakrishnan, R., Chokkanathan, U. & Geetha, K. Biological application and characterisation of Copper(II) complexes synthesised using Schiff base by an eco friendly method. *Int. J. Adv. Chem. Sci. Appl.* **3**(2), 10–15 (2015).
7. Vadivelmurugan, A., Sharmila, R., Pan, W.-L. & Tsai, S.-W. Preparation and evaluation of aminomalononitrile-coated Ca–Sr metal–organic frameworks as drug delivery carriers for antibacterial applications. *ACS Omega* **8**, 41909–41917. https://doi.org/10.1021/acsomega.3c06991 (2023).
8. Delehanty, J. B. et al. Antiviral properties of cobalt (III)-complexes. *Bioorg. Med. Chem.* **16**(2), 830–837. https://doi.org/10.1016/j.bmc.2007.10.022 (2008).
9. Karges, J. & Cohen, S. M. Metal complexes as antiviral agents for SARS-CoV-2. *ChemBioChem* **22**(16), 2600–2607. https://doi.org/10.1002/cbic.202100186 (2021).
10. Saleh, A. M., Abd El-Wahab, Z., Ali, O. A. M., Faheim, A. A. & Salman, A. A. Performance of new metal complexes for anionic and cationic dyes photodegradation: construction, spectroscopic studies, optical properties, and DFT calculations. *Res. Chem. Intermed.* **49**, 3287–3326. https://doi.org/10.1007/s11164-023-05049-9 (2023).
11. Nirmal Kumar, N., Prabakarakrishnan, R. & Geetha, K. Synthesis, characterisation and antimicrobial activity of binuclear manganese(II) complexes containing pentadentate schiff base ligand. *Int. J. Adv. Chem. Sci. Appl.* **3**(2), 37–42 (2015).
12. Climova, A. et al. Design of new Zn(II) pyrazine and pyridine derivatives based complexes as potential anticancer agents: from synthesis to structure. *Polyhedron* **245**, 116634. https://doi.org/10.1016/j.poly.2023.116634 (2023).
13. Ferjani, H., Smida, Y. B., Abdalla, A., Onwudiwe, D. C. & Hosten, E. Structural characterization, Hirshfeld surface analysis, optical properties, and DFT study of a new copper(II) complex. *Inorg. Chem. Commun.* **157**, 111314. https://doi.org/10.1016/j.inoche.2023.111314 (2023).
14. Natarajan, A. et al. In vivo evaluation of protective effect of Sargassum fusiforme on cisplatin induced hepato—renal toxicity. *Physiol. Mol. Plant Pathol.* **117**, 101748. https://doi.org/10.1016/j.pmpp.2021.101748 (2022).
15. Natarajan, A. et al. Hepato and renoprotective activity of Kappaphycus alvarezii ethanolic extract in cisplatin causes hepatic and kidney harm in Albino Wistar rats. *Aquacult. Int.* **31**, 1925–1940. https://doi.org/10.1007/s10499-023-01064-0 (2023).
16. Dinesh Karthik, A., Shakila, D., Geetha, K. & Muthuvel, I. Green approach to synthesize, spectral investigation and biological applications of potentially active ternary schiff base copper(II) complexes. *Mater. Today Proc.* **43**, 2389–2396. https://doi.org/10.1016/j.matpr.2021.02.135 (2021).
17. Geetha, K. & Chakravarty, A. R. Synthesis, crystal structure and properties of [Cu2(O2CC6H4Me-p)3-(Me2NCH2CH2NMe2)2] PF6: An unprecedented [Cu2(i-O2CR)4] into[Cu2(i-O2CR)3]1 core conversion. *J. Chem. Soc Dalton Trans.* **1**, 1623–1627. https://doi.org/10.1039/A900414I (1999).
18. Mukherjee, S. Solvent induced distortion in a square planar copper(II) complex containing an azo-functionalized Schiff base: Synthesis, crystal structure, in-vitro fungicidal and anti-proliferative, and catecholase activity. *J. Mol. Struct.* **1245**, 131057. https://doi.org/10.1016/j.molstruc.2021.131057 (2021).
19. Lakshmi, S. S., Geetha, K., Gayathri, M. & Shanmugam, G. Synthesis, crystal structures, spectroscopic characterization and in vitro antidiabetic studies of new Schiff base Copper(II) complexes. *J. Chem. Sci.* **128**(7), 1095–1102. https://doi.org/10.1007/s12039-016-1099-8 (2016).
20. Lakshmi, S. S., Geetha, K. & Mahadevi, P. Tridentate Schiff base (ONO) transition metal complexes: Synthesis, crystal structure, spectroscopic and larvicidal studies. *J. Chem. Sci.* **128**(7), 1113–1118. https://doi.org/10.1007/s12039-016-1107-z (2016).
21. Andiappan, K. et al. In vitro cytotoxicity activity of novel Schiff base ligand–lanthanide complexes. *Sci. Rep.* **8**, 3054. https://doi.org/10.1038/s41598-018-21366-1 (2018).
22. Abd El-Hamid, S. M., Sadeek, S. A., Mohammed, S. F., Ahmed, F. M. & El-Gedamy, M. S. Newly synthesised Schiff base metal complexes, characterisation, and contribution as enhancers of colon cancer cell apoptosis by overexpression of P53 protein. *Appl. Organomet. Chem.* **37**, e7129. https://doi.org/10.1002/aoc.7129 (2023).
23. Ram Kumar, A. et al. Spectroscopic, biological, and topological insights on lemonol as a potential anticancer agent. *ACS Omega* **8**, 31548–31566. https://doi.org/10.1021/acsomega.3c04922 (2023).
24. Aruna Kumar, S. Metallopharmaceuticals: Synthesis, characterization and bio-active studies. *Indian J. Biochem. Biophys.* **56**, 325–329 (2019).
25. Sanivarapu, A. K. Anti pathogenic studies of new mixed ligand metal chelates. *Indian J. Biochem. Biophy.* **59**, 189–196 (2022).
26. Praveen, S. et al. Theoretical Insights and Anticancer Potential of 2,6-Bis((*E*)-(2-amino-4-nitrophenylimino)methyl)-4-methoxyphenol and Its Binuclear Cu(II) Complex. *Appl. Organ. Chem.* **39**, e7984. https://doi.org/10.1002/aoc.7984 (2025).
27. Sinha, L. et al. FT-IR, FT-Raman and UV spectroscopic investigation, electronic properties, electric moments, and NBO analysis of anethole using quantum chemical calculations. *Spectrochim. Acta A* **133**, 165–177. https://doi.org/10.1016/j.saa.2014.05.034 (2014).
28. Kohn, W. & Sham, L. J. Self-consistent equations including exchange and correlation effects. *Phys. Rev.* **140**, A1133–A1138. https://doi.org/10.1103/PhysRev.140.A1133 (1965).
29. Becke, A. D. Density functional thermochemistry. III: The role of exact exchange. *J. Chem. Phys.* **98**, 5648–5652. https://doi.org/10.1063/1.464913 (1993).
30. Lee, C., Yang, W. & Parr, R. G. Development of the Colle-Salvetti correlation-energy formula into a functional of the electron density. *Phys. Rev. B* **37**, 785–789. https://doi.org/10.1103/PhysRevB.37.785 (1988).
31. Miehlich, B., Savin, A., Stoll, H. & Preuss, H. Results obtained with the correlation energy density functional of Becke and Lee. *Yang and Parr. Chem. Phys. Lett.* **157**(3), 200–206. https://doi.org/10.1016/0009-2614(89)87234-3 (1989).
32. Frisch, M. J., et al. Gaussion 09W, Revision A.02, Gaussion Inc. Walling ford, CT. gaussian.com/g09citation/ (2016).
33. Abdolmaleki, S., Panjehpour, A., Khaksar, S., Ghadermazi, M. & Rostamnia, S. Evaluation of central-metal effect on anticancer activity and mechanism of action of isostructural Cu(II) and Ni(II) complexes containing pyridine-2,6-dicarboxylate. *Eur. J. Med. Chem.* **245**(1), 114897. https://doi.org/10.1016/j.ejmech.2022.114897 (2023).
34. Ali, A. et al. Ligand substituent effect on the cytotoxicity activity of two new copper(II) complexes bearing 8-hydroxyquinoline derivatives: validated by MTT assay and apoptosis in MCF-7 cancer cell line (human breast cancer). *RSC Adv.* **11**, 14362–14373. https://doi.org/10.1039/D1RA00172H (2021).
35. Geary, W. J. The use of conductivity measurements in organic solvents for the characterisation of coordination compounds. *Coord. Chem. Rev.* **7**, 81–122. https://doi.org/10.1016/S0010-8545(00)80009-0 (1971).

36. Hazra, M., Dolai, T. & Pandey, A. Synthesis and characterisation of copper(II) complexes with tridentate NNO functionalized ligand: Density function theory study, DNA binding mechanism, optical properties, and biological application. *Bioinorg. Chem. Appl.* **104046**, 1–13. https://doi.org/10.1155/2014/104046 (2014).
37. Arjunan, V., Devi, L., Subbalakshmi, R., Rani, T. & Mohan, S. Synthesis, vibrational, NMR, quantum chemical and structure-activity relation studies of 2-hydroxy-4-methoxyacetophenone. *Spectrochim. Acta A Mol. Biomol. Spectrosc.* **130**, 164–177. https://doi.org/10.1016/j.saa.2014.03.121 (2014).
38. Andruh, M., Kahn, O., Sainton, J., Dromzee, Y. & Jeannin, S. Oxophily of gadolinium (III), and synthesis of dissymmetric di (Schiff bases) and dissymmetric dinuclear compounds. Crystal structure of [Cu2L'(OH)](ClO4) 2. cntdot. H2O with L'= 2-[N-(2-pyridylethyl) formimidoyl]-6-[N-((dimethylamino) propyl) formimidoyl] phenolato. *Inorg. Chem.* **32**, 1623–1628. https://doi.org/10.1021/ic00061a018 (1993).
39. Issa, Y. M., Hassib, H. B. & Abdelaal, H. E. 1H NMR, 13C NMR and mass spectral studies of some Schiff bases derived from 3-amino-1,2,4-triazole. *Spectrochim. Acta A Mol. Biomol. Spectrosc.* **74**(4), 902–910. https://doi.org/10.1016/j.saa.2009.08.042 (2009).
40. Venkatesh, R. & Geetha, K. Synthesis and spectroscopic investigation of novel nickel(II) complexes from pentadentate schiff base ligand. *SOJ Mater. Sci. Eng.* **3**(2), 1–5. https://doi.org/10.15226/sojmse.2015.00121 (2015).
41. Politzer, P. & Murray, J. S. The electrostatic potential: An overview. *WIREs Comput. Mol. Sci.* **1**(2), 153–163. https://doi.org/10.1002/wcms.19 (2011).
42. Thul, P., Gupta, V. P., Ram, V. J. & Tandon, P. Structural and spectroscopic studies on 2-pyranones. *Spectrochim. Acta A Mol. Biomol. Spectrosc.* **75**, 251–260. https://doi.org/10.1016/j.saa.2009.10.020 (2010).
43. Prasad, M. V. S., Udaya Sri, N. & Veeraiah, V. A combined experimental and theoretical studies on FT-IR, FT-Raman and UV–vis spectra of 2-chloro-3-quinolinecarboxaldehyde. *Spectrochim. Acta A Mol. Biomol. Spectrosc.* **148**, 163–174. https://doi.org/10.1016/j.saa.2015.03.105 (2015).
44. Kusmariya, B. S., Tiwari, A., Mishra, A. P. & Naikoo, G. A. Theoretical and experimental studies of Cu(II) and Zn(II) coordination compounds with N, O donor bidentate Schiff base ligand containing amino phenol moiety. *J. Mol. Struct.* **1119**, 115–123. https://doi.org/10.1016/j.molstruc.2016.04.056 (2016).
45. Gupta, V. P., Sharma, A., Virdi, A. & Ram, V. Structural and spectroscopic studies on some chloropyrimidine derivatives by experimental and quantum chemical methods. *Spectrochim. Acta A Mol. Biomol. Spectrosc.* **64**, 57–67. https://doi.org/10.1016/j.saa.2005.06.045 (2006).
46. Geetha, K., Nethaji, M., Chakravarty, A. R. & Vasanthacharya, N. Y. Synthesis, X-ray structure, and magnetic properties of ferromagnetically coupled binuclear copper(II) Complexes Having a (í-Hydroxo/methoxo)bis(í-benzoato)dicopper(II) Core. *Inorg. Chem.* **35**, 7666–7670. https://doi.org/10.1021/ic9607550 (1996).
47. Aprajita, M. C. Synthesis and characterization of phenoxy-bridged copper(II) complexes: Structural features, magnetic, thermal and redox properties, and theoretical studies. *Inorg. Chim. Acta* **557**, 121708. https://doi.org/10.1016/j.ica.2023.121708 (2023).
48. Prabakarakrishnan, R. et al. Computational and experimental studies of Metallo organic framework on human epidermal cell line and anticancer potential. *Environ. Res.* **201**, 111520. https://doi.org/10.1016/j.envres.2021.111520 (2021).
49. Ayoub, M. A., Abd-Elnasser, E. H., Ahmed, M.A.-A. & Rizk, M. G. Synthesis, physicochemical, thermal, fluorescence and catalytic activity studies of novel Mn (II), Co (II), Ni (II) and Cu (II) complexes with tridentate (ONS) Schiff base ligand. *Eur. J. Chem.* **8**, 85–95. https://doi.org/10.5155/eurjchem.8.1.85-95.1513 (2017).
50. Biswas, N. et al. One new azido bridged dinuclear copper (II) thiosemicarbazide complex: synthesis, DNA/protein binding, molecular docking study and cytotoxicity activity. *New J. Chem.* **41**, 12996–13011. https://doi.org/10.1039/C7NJ01998J (2017).
51. Singh, N. K., Kumbhar, A. A., Pokharel, Y. R. & Yadav, P. N. Anticancer potency of copper(II) complexes of thiosemicarbazones. *J. Inorg. Biochem.* **210**, 111134. https://doi.org/10.1016/j.jinorgbio.2020.111134 (2020).
52. Qin, Q.-P., Tan, B.-Q.-X., Wang, S.-L., Liu, Y.-C. & Liang, H. Tryptanthrin derivative copper(II) complexes with high antitumor activity by inhibiting telomerase activity, and inducing mitochondria-mediated apoptosis and S-phase arrest in BEL-7402. *New J. Chem.* **42**, 15479–15487. https://doi.org/10.1039/C8NJ03005G (2018).
53. Sankar, R. & Sharmila, T. M. Schiff bases-based metallo complexes and their crucial role in the realm of pharmacology A review. *Res. Chem.* **6**, 101179. https://doi.org/10.1016/j.rechem.2023.101179 (2023).

Acknowledgements

I am very much grateful my research supervisor, Dr. K. Geetha, Associate Professor & Head, PG and Research Department of Chemistry, Muthurangam Govt. Arts College, Vellore, Tamilnadu, India, for the unwavering support and encouragement during the research. The author is thankful for the financial support rendered by Department of Science and Technology, India by the sanction order 100/IFD/5126/2009-2010. This project was supported by Researchers Supporting Project number (RSP2025R383), King Saud University, Riyadh, Saudi Arabia. Author SK acknowledged the Department of Science and Technology for the equipment support under the DST FIST (PG Colleges) Level A Scheme (Sanction No. SR/FST/COLLEGE-/2022/1293 dated 19-12-2022).

Author contributions

Conceptualization: S. Praveen, R. Prabakarakrishnan, Methodology: G. Parinamachivayam, A. Natarajan, Data Collection/Investigation: Elumalai Perumal Venkatesan, K. Geetha, Data Analysis: Arunachalam Chinnathambi, Sulaiman Ali Alharbi, Writing—Original Draft: K. Geetha, Writing—Review & Editing: Arivalagan Pugazhendhi, Sabariswaran, Kandasamy, Nasim Hasan.

Declarations

Competing interests

The authors declare no competing interests.

Additional information

Correspondence and requests for materials should be addressed to K.G. or N.H.

Reprints and permissions information is available at www.nature.com/reprints.

Publisher's note Springer Nature remains neutral with regard to jurisdictional claims in published maps and institutional affiliations.